Comments from Reviewer 2:

This manuscript studies the interannual variability of shelf circulation in the Northern South China Sea (NSCS). Low-frequency variability in the ENSO and the Pearl River Estuary (PRE) runoff are shown to have important effects in the spatial patterns of cross-isobath transport. Distinct regimes exist inshore and offshore of the 100 m isobath, respectively associated with bottom friction+nonlinear effects and stratification-dominated effects. The regions east and west of the PRE's outflow are also starkly different, being respectively dominated by variability in the PRE plume's volume and in the Kuroshio's intrusions.

The text, figures and tables could use minor improvements but read generally well, and the reasoning is easy to follow. The major issues I see with the manuscript are in terms of a couple of subjective choices, namely the regression analysis methodology and the criterion for identifying large-outflow years.

Response: We appreciate the reviewer's thoughtful comments on our work. We have taken your concerns into account and have made the appropriate revision following your suggestions.

Major points:

M1 (lines 218-229): I am not sure I follow the need for the regression step in the two-stage regression approach. My understanding is that this analysis is a conditional average of the anomaly fields for each variable at the times when each variable's MVPC1/PC1 was in a positive phase, is that correct? I do not follow where the linear slopes calculated from the least-squares analysis are actually used. The time series of the MVPC1/PC1 should contain the relevant temporal variability of the leading EOF mode. Please clarify this paragraph.

To justify the need for a more elaborate method, the authors also need to compare it to the simplest one. How do all results in the paper compare to doing the same analyses

just by conditionally-averaging the anomaly fields over years of positive MVPC1/PC1 phase?

Response: We appreciate the request to clarify the role of the regression step. Our aim is to (i) extract the spatial pattern linked to the leading coupled mode and (ii) present a representative positive-phase amplitude with reduced year-to-year noise. Concretely, we regress each anomaly field on the standardized MVPC1/PC1; the resulting slope map is an effect size per +1 s.d. of the mode. For display, we scale that slope by the mean positive-phase amplitude to form the plotted "positive-phase" pattern. Thus, the regression slopes are directly used to construct the maps and quantify amplitudes.

Following the reviewer's suggestion, we also computed simple conditional averages of the raw anomalies over positive-phase summers. These maps closely resemble the regression-scaled patterns, with only small coastal differences. We now note this agreement in the text and provide a short side-by-side panel in the Supplement.

In the revised manuscript, we include these information as:

To characterize interannual anomalies in shelf currents and hydrography, we use a regression-scaled composite. First, for each variable, we regress its anomaly field on the standardized MVPC1/PC1 (Fig. 3g,h). The resulting slope map is an effect size—anomaly per +1 standard deviation of the mode—that uses all years and reduces synoptic noise. To depict the positive phase, we scale this slope by the mean of the index during summers when the index is positive (years in Tables 1 – 2), which is numerically close to a simple conditional average but provides a directly interpretable amplitude and enforces phase antisymmetry. For transparency, we also compute simple conditional-average maps; these closely match the regression-scaled patterns (Fig. S2), and we therefore retain the regression-scaled maps in the main text for consistency across variables.

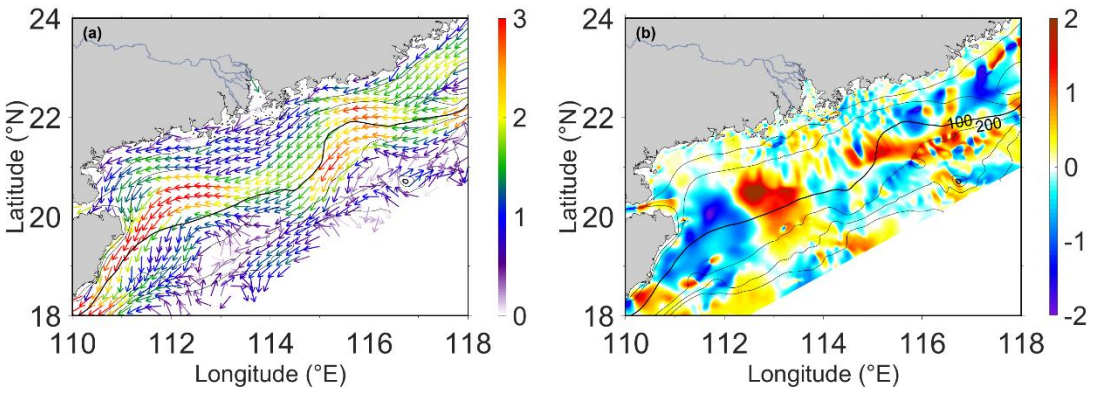

Figure S2. (a) Mean velocity vector anomalies (cm s^{-1}), and (b) mean cross-isobath velocity anomalies (cm s^{-1}) during summer in positive MVPC1 years (Table 1).

M2 (line 197-199): Is there an objective criterion for choosing large-runoff years, like an outflow volume threshold? I think it is important to have one, and it should be described here.

Because the choice of the threshold is also arbitrary (e.g., it could be the years where the outflow was greater than the 75th or 90th percentile), a second step is to study the sensitivity of the results to this choice as well.

Response: We appreciate this suggestion. We now define large-runoff years using a simple percentile rule. For each year y, we compute the summer-mean Pearl River discharge $Q(y)$. Years with $Q(y) \geqslant Q_p$ are classified as high-runoff, where we use p=70% as a reference choice. In our record (2000–2022) this corresponds to 26,000 m^3 s^{-1}, yielding **7** high-runoff and **6** low-runoff summers. To assess sensitivity, we repeat the key composites and regressions for p=80%. The principal spatial features and interpretations are generally similar across thresholds, with some variations in amplitude as expected. We also compare this percentile rule with the sign of the SSS-EOF PC1 and find substantial overlap. These details are described in Methods and summarized in Fig. S1.

In the revised Supplement, we included:

The large-runoff years are identified by a simple percentile rule: for each year we

compute the summer-mean Pearl River discharge $Q(y)$, and label years with $Q(y) \geq Q_{70\%}$ as high-runoff. Over 2000–2022, this threshold equals 26,000 m³ s⁻¹. Figure S1 shows that raising the cutoff to $Q_{80\%}$ produces almost the same spatial patterns with only minor amplitude differences, which confirms that $Q_{70\%}$ is sufficient to distinguish between large- and low-runoff years.

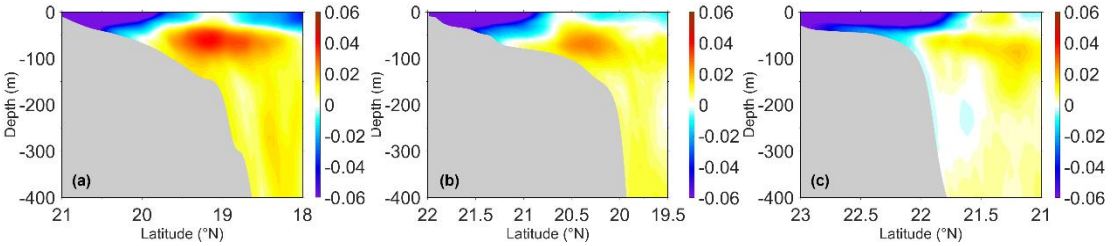

Figure S1. (a) Salinity anomaly profiles (psu) during summer in years exceeding the 80% runoff threshold (Table 2) at Transect A; (b) salinity anomaly profiles during summer in years exceeding the 80% runoff threshold at Transect B; (c) salinity anomaly profiles during summer in years exceeding the 80% runoff threshold at Transect C.

M3: I think a key result worth emphasizing is the identification of the different dynamical regimes in terms of their response to different ENSO/PRE plume drivers (inshore PGF_{y*}^b-dominated/offshore JEBAR-dominated and west Kuroshio intrusion-dominated/east PRE plume-dominated). I think adding a schematic/cartoon-type figure illustrating these would be a good way to summarize the results in a mechanistic way and make them more visible to readers studying other regions influenced by Western Boundary Currents, wind-driven upwelling, and large river outflows.

Response: We appreciate the suggestion. We have added a concise schematic that summarizes the summer dynamical regimes identified in our analyses (new Fig. 10). The schematic highlights (i) an inshore branch where bottom pressure-gradient forcing dominates cross-isobath transport, (ii) an outer-shelf/slope branch where JEBAR is predominant, and (iii) a west–east contrast between a

Kuroshio-intrusion-influenced western sector and a PRE-plume-influenced eastern sector. We also indicate the sign of the anomalies associated with ENSO phase and with high/low discharge in a qualitative way to avoid visual clutter. This figure is intended as a compact, mechanistic summary for readers and complements the quantitative maps and budgets in the main text.

In the revised manuscript, we included:

Figure 10 delineates the regions of dominance exerted by the primary drivers: runoff and ENSO (PGF^{b}_{y*} and JEBAR) during summer in the NSCS, and the main influencing factors are basically arranged from the shore to the open ocean as runoff, PGF^{b}_{y*}, and JEBAR.

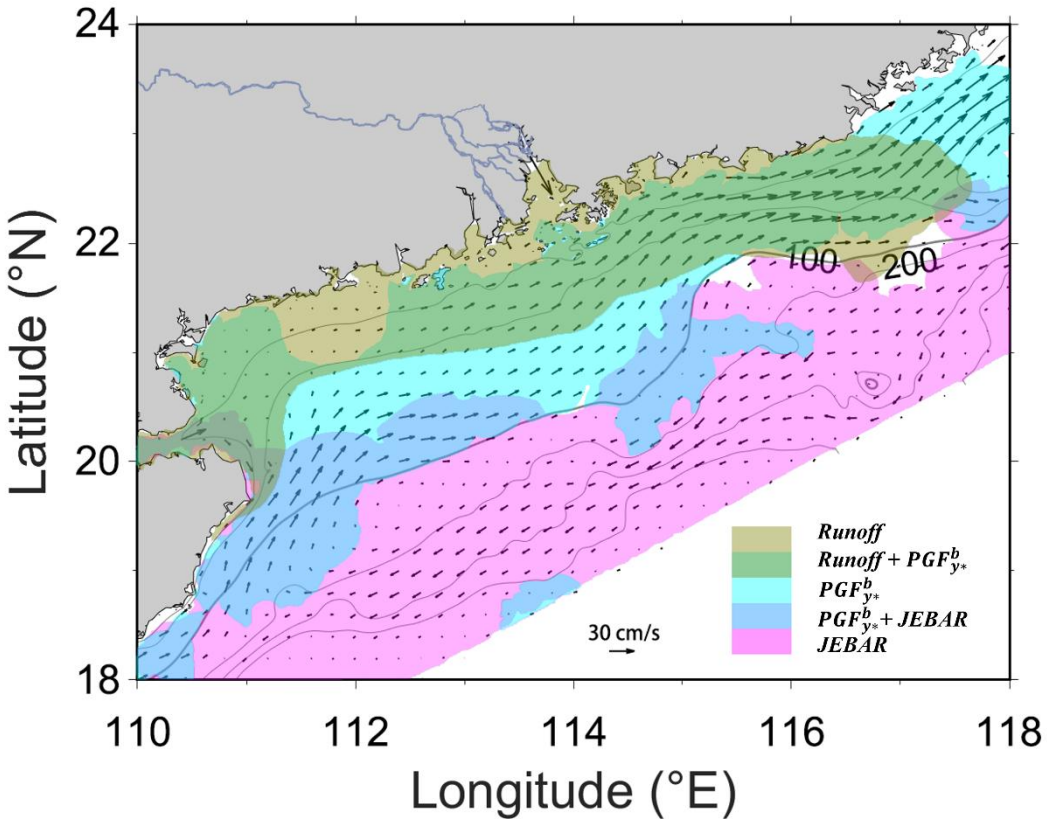

Figure 10. Schematic map of the regions controlled by different impact factors (*Runoff*, PGF^{b}_{y*} and *JEBAR*) during summer in the NSCS. The arrows depict the mean summer shelf circulation.

Minor points

m1 (lines 39-41): Topographic effects should be more important in locations with more curved isobaths such as in the NSCS' widened shelf area, as previous work in the NSCS shows. So I don't follow why nearly shore-parallel isobaths should result in enhanced cross-isobath flow.

Response: We apologize for any confusion caused by the ambiguous expression. This sentence has been rewritten for clarity in the revised version. The last sentence of the introduction section now reads:

" In addition to wind-driven Ekman transport, cross-isobath exchanges are strongly influenced by topographic effects, which mainly function over the concave shelf where the isobaths show spatial irregularity (Liu et al., 2020)."

m2 (lines 82 and 119): Comparing the model resolution to the local first deformation radius derived from the model stratification is important here, especially inshore of the 100 m isobath (where the nonlinear terms are shown to be more important in the depth-averaged vorticity balance).

Response: The local first deformation radius inshore of the 100 m isobath (apart from the coastal area) ranges from a few to ~10 km, which is sufficiently larger than the model resolution yet at least an order of magnitude smaller than the shelf width, so the nonlinear terms likely play only a minor role in the depth-averaged vorticity balance.

In the revised manuscript, we included at end of section 3.2:
It is also noteworthy from this figure that landward of the 100-m isobath (excluding the immediate nearshore), the first baroclinic Rossby radius exceeds the model grid spacing yet remains an order of magnitude smaller than the shelf width, supporting the validity of the climatic scales adopted in this study.

m3 (line 87): A couple of example references using the Mellor-Yamada scheme could be added here, in addition to the original paper describing the scheme.

Response: Two representative papers (Gan et al., 2006; Jing et al., 2009) employing the Mellor–Yamada scheme for South China Sea circulation modeling have now been cited in the revised manuscript.

m4 (Fig 1): It would be helpful to add the 100 m and 200 m isobaths to this figure for reference. In Figs. 4, 6, and A1, it would also help to have them labelled on the figure itself.

Response: Thanks for this important reminder. We have added the isobaths and labels in the figures of the revised manuscript.

Such as Figure 1:

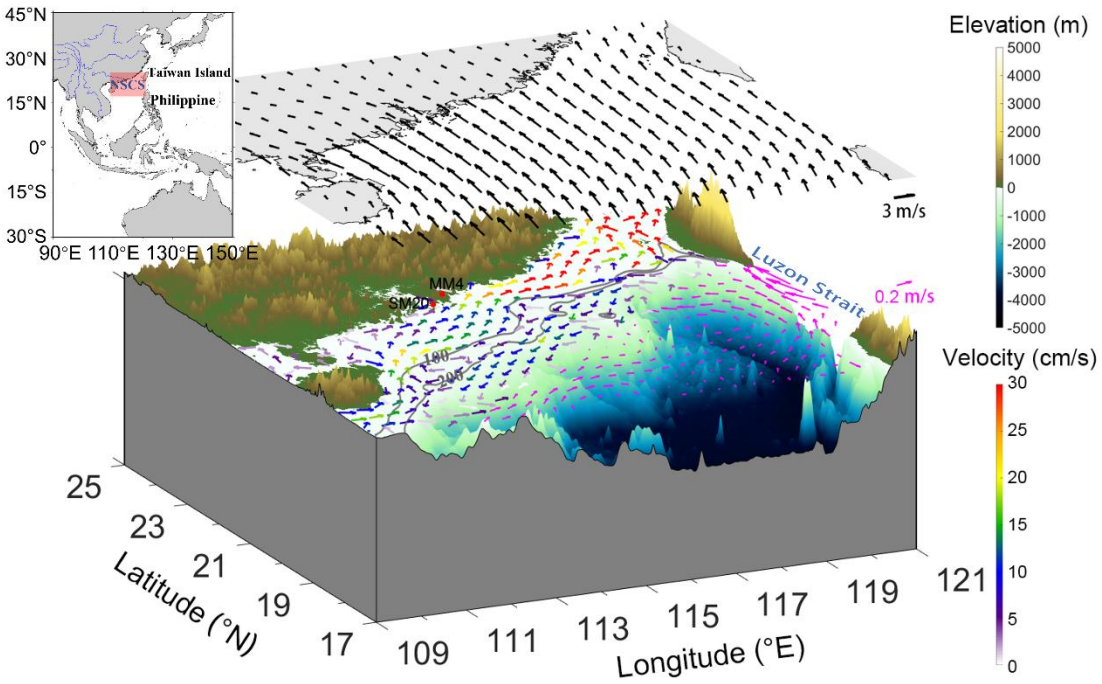

m5 (Fig 1's caption): Are the geostrophic currents shown as pink arrows the surface

geostrophic velocity derived from the model sea surface slopes? This could use clarification. Differentiating between "geostrophic" and "shelf" currents is also confusing because there are geostrophic currents both on the shelf and offshore.

Response: The geostrophic currents outside the model domain are derived from CMEMS satellite products. A clearer statement has been added to the revised manuscript. The caption of Fig. 1 now reads:

"Figure 1. Overview map of the northern South China Sea. Model-simulated shelf currents (colored arrows) within the model domain and satellite-derived geostrophic currents (pink arrows) outside the scope of the model simulation represent summer averages from 2000 to 2022. The upper panel shows the corresponding climatological wind field. Red markers indicate the observational sites used for model validation in Fig. 2. The upper left sub-graph shows the location of the northern South China Sea."

m6 (line 247): How are the degrees of freedom estimated (e.g., from integral timescales derived from the time series of the velocity components at each grid point)? It would be good to describe it here.

Response: The degrees of freedom estimated are automatically computed by the MATLAB toolbox. For the simple linear regression $Y = \beta_0 + \beta_1 X + \varepsilon$ with N observations, the model estimates two parameters (intercept and slope). Consequently, the residual degrees of freedom are N-2. The caption of Fig. 4 now reads:

"Figure 4. Depth-averaged circulation and associated anomalies in the northern South China Sea: (a) mean velocity vectors (cm s^{-1}) and (b) mean cross-isobath velocity (cm s^{-1}) averaged over summers from 2000 to 2022, where positive cross-isobath velocity indicates flow from deeper to shallower waters; (c) regression map of velocity vector anomalies (cm s^{-1}), and (d) regression map of cross-isobath velocity anomalies (cm s^{-1}) during positive MVPC1 years (Table 1). Shaded areas in (c) and (d) denote regions where the 90% confidence level is not met, based on a two-tailed t-test using

the estimated standard deviation and sample degrees of freedom. For the simple linear regression, the degrees of freedom are N-2 (N is the number of observations). The two-stage regression approach is detailed in Section 3.2. Positive values in (c) and (d) indicate flow toward shallower waters."

m7 (Fig. 5) The discussion relies on different stratification regimes, which appear to be both salinity- and temperature-driven. It would therefore help to overlay isopycnals of the conditionally-averaged density fields on each panel.

Response: Thanks for your suggestion. We have now overlaid contour lines of the regressed density anomaly on each panel in the revised Fig.5:

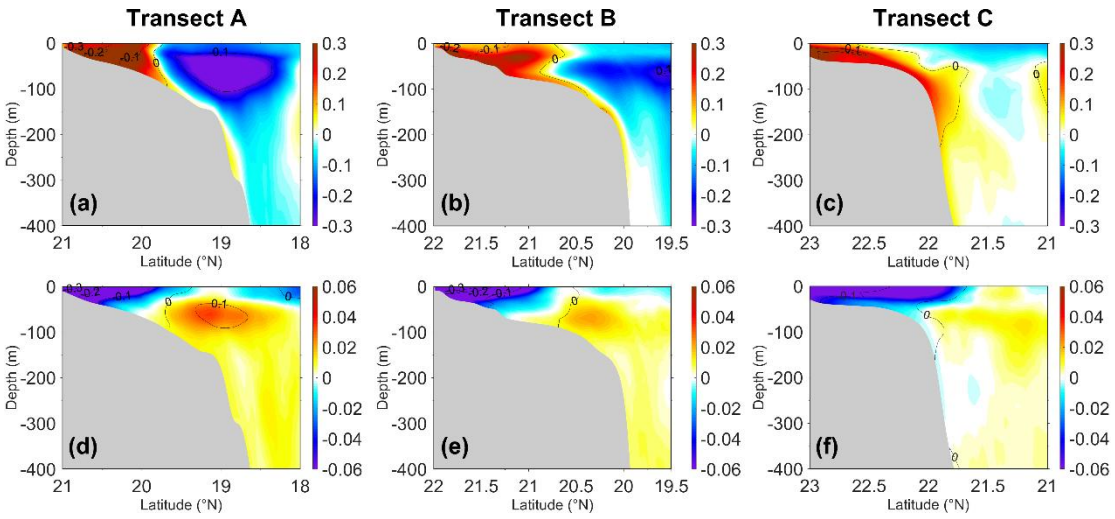

Figure 5. Regression maps of hydrographic anomalies along three cross-shelf transects (locations shown in Fig. 4b): (a–c) temperature anomaly profiles (°C) during positive MVPC1 years (Table 1) at Transects A, B, and C, respectively; (d–f) salinity anomaly profiles (psu) during positive PC1 years (Table 2) at the same transects. The isolines depict the regressed density anomalies for the corresponding scenarios. The two-stage regression approach is detailed in Section 3.2.

m8 (line 290-291): It is more objective to include some metric of the smallness of the

GMF term, for example, what is its size relative to the next-largest term in the balance? This ratio will also vary spatially, so I suggest the authors include a figure with the GMF term's spatial structure and its relative size in the Appendix.

Response: Thanks for your suggestion. A figure illustrating the contribution of the GMF term (Fig. S3) has been added to the revised manuscript.

In the revised Supplement, we included:

The spatial structure of the cross-isobath velocity anomaly contributed by the term GMF during positive MVPC1 years is displayed in Fig. S3. Its magnitude is negligible compared with the other terms (except within the PRE). Therefore, it is reasonable for us to omit the discussion of this item in the main text.

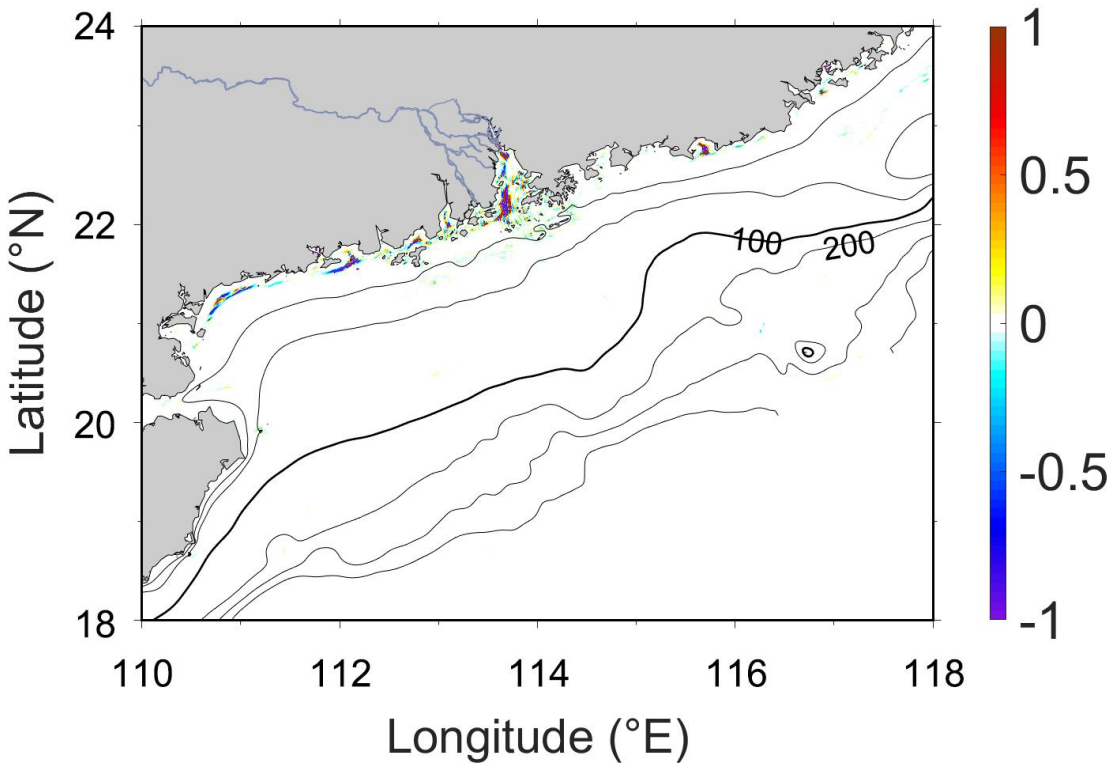

Figure S3. Regression maps of horizontal cross-isobath velocity anomalies (cm s^{-1}) during positive MVPC1 years (Table 1), attributed to the gradient of momentum flux (GMF).

m9 (Fig. 8 caption): Are these each of the JEBAR terms' contributions to the total PGF_{y*}^b/f anomalies in cm/s (like Fig. 6)? Please add the units to the caption like in Fig. 6, or to the colorbar labels.

Response: All items in Fig.8 were calculated independently and should be expressed in $m^2\ s^{-2}$. This unit has now been included in the figure caption in the revised manuscript. The caption of Fig. 8 now reads:

"**Figure 8.** Regression maps of horizontal components ($m^2\ s^{-2}$) in the JEBAR term during summer and positive MVPC1 years, under different runoff conditions: (a–c) correspond to positive PC1 years, and (d–f) to negative PC1 years. Panels show (a, d) the full baroclinic gradient term ($\frac{g}{\rho_0}\int_{-H}^{0} z(\rho-\bar{\rho})dz$), (b, e) the contribution from vertical density stratification ($-\frac{g}{\rho_0}\int_{-H}^{0}\frac{z^2}{2}\frac{\partial(\rho-\bar{\rho})}{\partial z}dz$), and (c, f) the contribution from bottom density anomaly ($-\frac{g}{\rho_0}\frac{H^2}{2}(\rho-\bar{\rho})_b$). The MVPC1 time series is shown in Fig. 3g, with corresponding positive-phase years listed in Table 1, while the PC1 time series is shown in Fig. 3h with its positive-phase years listed in Table 2. The two-stage regression approach is detailed in Section 3.2."

Typos/minor edits

Line 23: Intrusion -> intrusions

Line 91: Large amount of freshwater influx -> a large freshwater influx

Line 119: Smaller scaled -> smaller-scale

Line 119: Could be further detailed -> are not fully resolved

Line 196: Streamflow -> runoff/outflow

Line 214: Missing space before "Interannual"

Line 294: Within the -> inshore of

Line 377: In the -> in

Response: All corrections have been applied in the revised manuscript.

References:

Gan J., Li H., Curchitser E. N., and Haidvogel D. B.: Modeling South China Sea circulation: Response to seasonal forcing regimes, Journal of Geophysical Research: Oceans, 111(C6). doi:10.1029/2005JC003298, 2006.

Jing Z., Qi Y., Hua Z., and Zhang H.: Numerical study on the summer upwelling system in the northern continental shelf of the South China Sea, Continental Shelf Research, 29(2): 467–478, doi:10.1016/j.csr.2008.11.008, 2009.